Multiple valued floating potentials of Langmuir probes

Cheol-Hee Nam, N. Hershkowitz, M. H. Cho, T. Intrator, and D. Diebold[a)]
Department of Nuclear Engineering and Engineering Physics, University of Wisconsin-Madison, Madison, Wisconsin 53706

(Received 30 November 1987; accepted for publication 15 February 1988)

It is shown that Langmuir probes can have three different floating potentials in plasmas produced by a hot filament discharge in a multi-dipole device when the primary and secondary electron currents are comparable. The measured floating potential depends on the probe's initial condition—the most negative and the least negative potentials are found to be stable and the in-between value is found to be unstable. Results are compared to a simple theoretical model.

I. INTRODUCTION

The floating potential of a Langmuir probe in a plasma is the bias potential at which a probe draws no net current, i.e., electron and ion currents balance. It is relatively easy to measure the floating potential requiring little more than a high impedance voltmeter, if frequency response is not an issue. It is often taken to be a good indicator of the plasma potential.[1,2] For nondrifting Maxwellian plasmas with electron temperature T_e, it is easy to show that the floating potential differs from the plasma potential by several T_e/e.[1,2]

Many plasmas contain electrons and/or ions which are sufficiently energetic to produce secondary electrons. It has been recognized that secondary electron emission from a probe can reduce the apparent electron temperature and shift the floating potential[3] because the emitted secondary electron current looks like an effective collected ion current. In this paper we show that the secondary electron emission can result in a more extreme phenomena—multiple valued floating potentials. Here we give an example of a probe which can draw zero net current for three bias voltages in the same plasma. We also show that two of the floating potentials are stable and the other one is unstable for the same plasma.

II. EXPERIMENTAL CONSIDERATION

The experiment was performed in a multi-dipole plasma device[4,5] which has 14 vertical and six top and eight bottom magnet arrays. These magnet arrays form a surface magnetic field near the chamber wall so that the plasma is formed in a magnetic-field-free region. Argon plasma was produced by energetic primary electrons emitted from hot filaments. Typical plasma parameters were electron temperature $T_e = 2$–6 eV, ion temperature $T_i \simeq 0.2$ eV, and electron density $n_e = 3\times 10^8$–4×10^9 cm^{-3} with the argon neutral pressure $P_0 = 1\times 10^{-5}$–4×10^{-4} Torr. The plasma forms a virtual anode concentric with each filament so that the energy of the primary electron E_p is determined by the plasma potential minus the filament bias, i.e., $E_p = e(V_p - V_F)$, where V_p is the plasma potential and V_F is the filament bias voltage. The primary ionizing electrons are confined by the multidipole magnetic field. This confinement of primary electrons significantly increases the plasma density[4–6] compared to devices without surface magnetic fields. The primary electron distribution function can be represented by a shell in velocity space.[5]

The primary electrons cause the emission of the secondary electrons from the probe. If the secondary electron emission is not restricted by a space charge, the secondary electrons leave the probe freely.[7] The secondary electron emission yield $\sigma(E)$ is defined as the average number of secondary electrons emitted from a bombarded material for every incident primary electron.[8] For a clean tantalum $\sigma(E)$ has a value of unity at $E_p = 250$ eV and a maximum value of $\sigma_m \simeq 1.3$ at $E_p = 600$ eV.[8–10] The secondary electron emission yield $\sigma(E)$ of clean tantalum varies almost linearly from 20 to 400 eV.[9] For the measurements of the secondary electron emission effects on the Langmuir probe *I-V* characteristic presented here, 5- and 0.6-cm diam tantalum disks were used.

III. EXPERIMENTAL RESULTS

The floating potentials of probes measured by a typical voltmeter (1-MΩ impedance) as a function of the primary electron energy are shown in Fig. 1 (for the 0.6-cm diam tantalum disk) and Fig. 2 (for the 5-cm diam tantalum disk). The discharge current was kept constant during the measurement in each case. When the primary electron energy E_p is increased, the floating potential becomes more negative to repel the increased electron energy. When the secondary electron current, which contributes a positive current, is greater than the primary electron current, the floating potential is expected to become more positive. In Fig. 2 it is seen that the floating potential of the larger diameter probe jumps positively above a certain critical energy of the primary electron. This sudden jump of the floating potential is explained later. When E_p is large enough, the primary and secondary electron currents severely affect the Langmuir probe *I-V* characteristic.

When the primary electron energy is greater than the critical energy and the neutral pressure is low, the Langmuir probe *I-V* characteristic was found to have three different floating potentials. Although the Langmuir probe *I-V* characteristic has three different floating potentials, the voltmeter indicated only the least negative potential. Above the critical energy the measured floating potential jumped positively. On the other hand, the measured floating potential of

[a)] Present address: U.S. Department of Energy, Washington, DC.

 0021-8979/88/125674-04$02.40

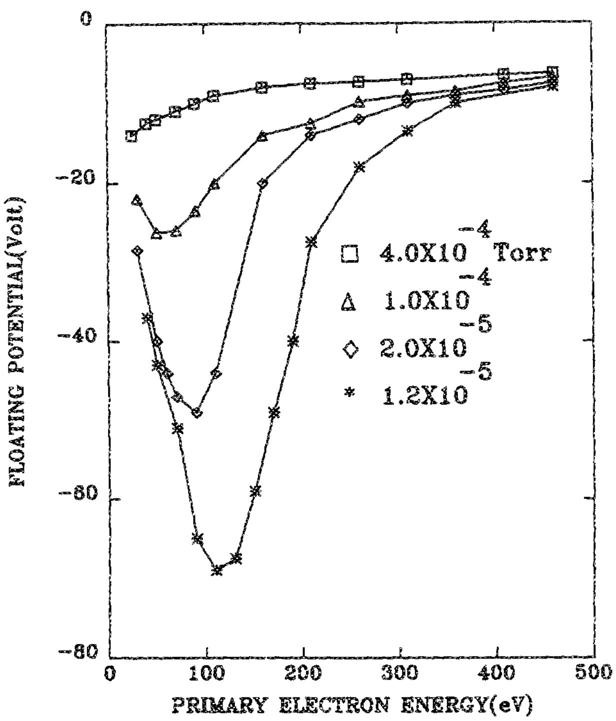

FIG. 1. Primary electron energy vs floating potential measured by a 0.6-cm diam tantalum disk probe. The discharge current is fixed at 100 mA.

the 0.6-cm tantalum disk probe does not show the jump of the floating potential.

The data in Fig. 3 show why the 0.6-cm tantalum disk probe does not show the discontinuous jump. The current scale is normalized by the collecting area of the probe in Fig. 3. The area ratio of the 5-cm tantalum disk probe to the 0.6-cm tantalum disk is about 70 so that the slope of the load line

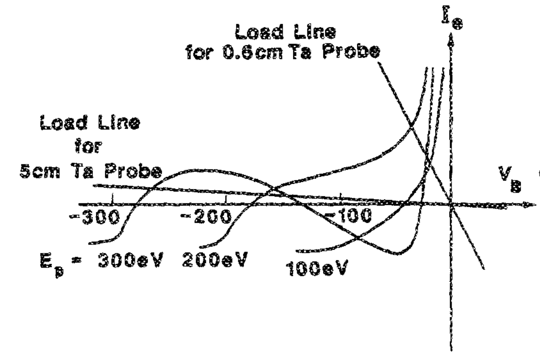

FIG. 3. The Langmuir probe *I-V* characteristics and the load line of measuring circuit for 0.6- and 5-cm tantalum disk probes. The load lines are normalized by the collecting area of probe. The scale is exaggerated for illustration.

for the 0.6-cm tantalum disk probe is 70 times greater than that of the 5-cm tantalum disk probe. The *I-V* characteristic has three different floating potentials, i.e., three intersections with $I = 0$, the load line with zero slope. The load line for the 5-cm tantalum disk probe has three crossing points with *I-V* characteristic but the load line for 0.6-cm tantalum disk probe has only one crossing point. Note that the 1-MΩ input impedance of the voltmeter is not large enough to accurately measure the two floating potentials of the 0.6-cm tantalum disk probe in this case and then the least negative potential is indicated.

Langmuir probe *I-V* characteristics for various conditions are shown in Fig. 4. At high neutral pressures the Langmuir probe *I-V* characteristic does not have multiple valued floating potentials because the primary electron and secondary electron currents are smaller than plasma ion current.

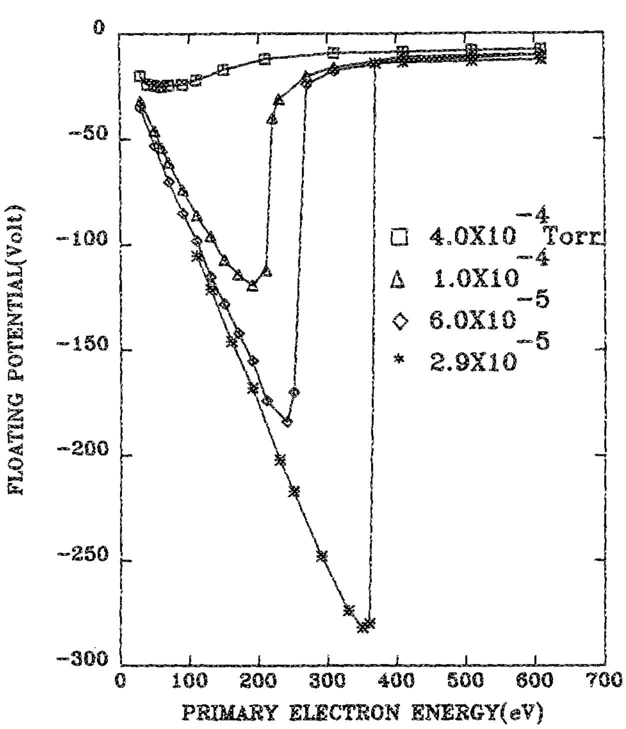

FIG. 2. Primary electron energy vs floating potential measured by a 5-cm diam tantalum disk probe. The discharge current is fixed at 100 mA.

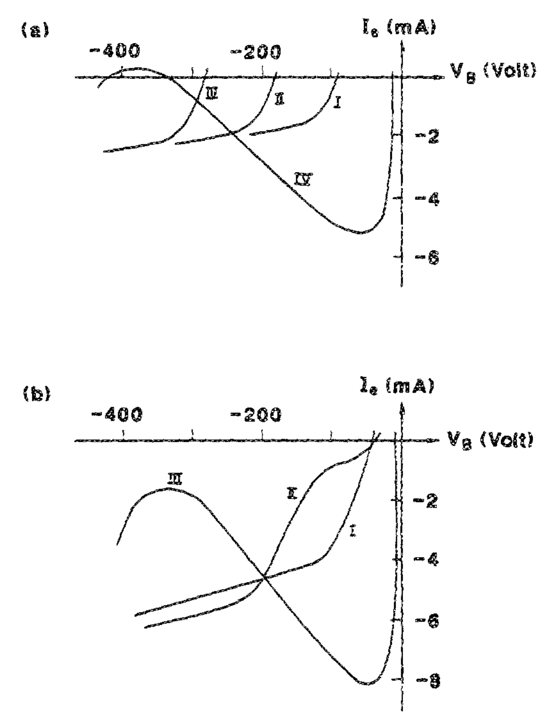

FIG. 4. *I-V* characteristics of a 5-cm diam tantalum disk probe. (a) I. $E_p = 100$ eV, II. 200 eV, III. 300 eV, IV. 400 eV with $P_0 = 1\times10^4$ Torr. (b) I. $E_p = 100$ eV, II. 200 eV, III. 400 eV with $P_0 = 4\times10^{-4}$ Torr.

The measured floating potential was found to depend on the initial condition of the probe—the most negative and least negative potentials were found to be stable and the in between one to be unstable. If the probe was initially biased more negative than the in between potential ϕ_{f2}, the floating potential is ϕ_{f1}. Otherwise the floating potential is ϕ_{f3}.

IV. DISCUSSION

A. The reason for two stable values of floating potential

Note that at ϕ_{f1} and ϕ_{f3} the I-V characteristics have a negative slope, i.e., $dI/dV<0$, and at ϕ_{f2} it has a positive slope, i.e., $dI/dV>0$ (see Fig. 5). If the probe is floating at either ϕ_{f1} or ϕ_{f3} and the potential is perturbed positively, negative current flows through the capacitance between the probe and ground. The negative current decreases the voltage across the capacitor and the positive perturbation is reduced. If the potential is perturbed negatively from ϕ_{f1} or ϕ_{f3}, the voltage across the capacitor is increased by the positive current and the perturbation is again reduced. Therefore, these two potentials are stable.

If the probe is floating at ϕ_{f2} and the potential is perturbed positively, then the voltage across the capacitor is increased by the positive current. The increased voltage causes more positive current so that the voltage is increased more positively until it reaches the stable floating potential ϕ_{f3}. When the potential is perturbed negatively, a similar process drives the potential to the stable floating potential ϕ_{f1}. Therefore, ϕ_{f3} results from the initial probe bias above ϕ_{f2} while ϕ_{f1} from an initial probe bias below ϕ_{f2}.

B. Simple theoretical model

The current collected by a probe is composed of ion and electron currents, and primary and secondary electron currents. The probe current I_{pl} from the background electrons and ions with Maxwellian distributions is expressed[1,2] by

$$I_{pl}(V_B) = I_{is} - n_e eA\sqrt{(T_e/2\pi m_e)} \times \exp[-e(V_p - V_B)/T_e], \quad V_B \leqslant V_p, \tag{1}$$

where I_{is} is the ion saturation current, A is the collecting area of the probe, and V_B is the probe bias voltage. The primary electron emitted from the hot filament can be considered to be monoenergetic, i.e., a shell distribution in the velocity space. The primary electron current I_{ep} as a function of the probe bias can be written[5,11]

$$I_{ep}(V_B) = -(n_{ep}eAv_{ep}/4) \times\{1-[e(V_p - V_B)/E_p]\}, \tag{2}$$

where v_{ep} is the velocity of primary electrons and n_{ep} is the primary electron density. Note that the primary electron current varies linearly with the probe bias V_B. In order to simplify the calculation of the secondary emission current, we assume that the secondary emission yield $\sigma(E)$ has a following form:

$$\sigma(E) = a + b(E/E_0), \quad \text{for } E \geqslant 20 \text{ eV}, \tag{3}$$

where $a = 0.43$, $b = 0.82$, and $E_0 = 400$ eV for a clean tantalum. This expression is valid within $\pm 6\%$ for $E_p \leqslant 400$ eV.[9] The secondary electron current I_{es} as a function of the probe bias V_B can be written[12]

$$I_{es}(V_B) = \frac{2\pi eA}{m_e^2}\int f(\epsilon)\epsilon\left(1 - \frac{e(V_p - V_B)}{\epsilon}\right) \times \sigma[\epsilon - e(V_p - V_B)]\, d\epsilon, \tag{4}$$

where $\epsilon = m_e v^2/2$ and $f(\epsilon)$ is the velocity distribution function with v replaced with $\sqrt{2\epsilon/m_e}$ of the primary electron. For monoenergetic primary electrons the distribution function is given by

$$f(\epsilon) = (n_{ep}m_e/4\pi v_{ep})\delta(\epsilon - E_p). \tag{5}$$

Substituting Eqs. (3) and (5) into Eq. (4) and carrying out integral gives

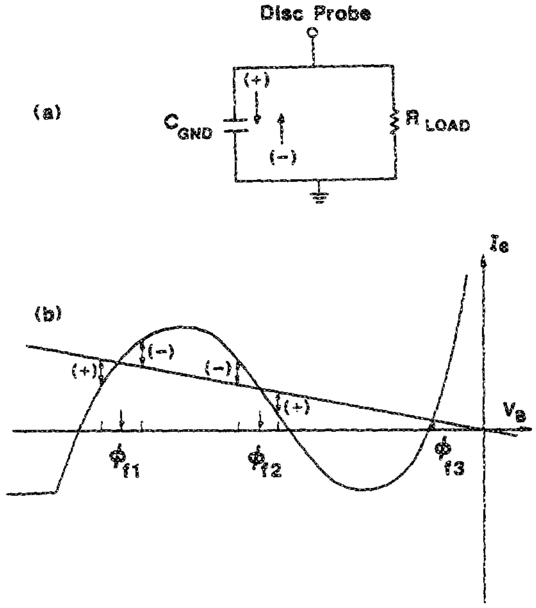

FIG. 5. (a) Equivalent circuit diagram for the floating potential measuring circuit, and (b) the load line for the circuit. The scale is exaggerated for illustration.

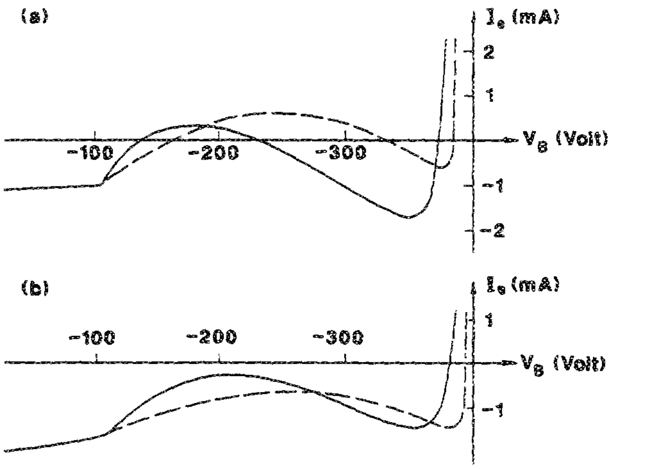

FIG. 6. Comparison of the experimental data and theoretical I-V characteristics. The solid lines indicate the experimental data and the dotted lines the theoretical calculation. (a) $T_e = 6$ eV, $n_e = 6.9\times10^8$ cm^{-3}, $P_0 = 2\times10^{-5}$ Torr. (b) $T_e = 4$ eV, $n_e = 1.3\times10^9$ cm^{-3}, $P_0 = 4\times10^{-5}$ Torr.

$$I_{es}(V_B) = \frac{n_{ep} e A v_{ep}}{4} \left[a \left(1 - \frac{e(V_p - V_B)}{E_p} \right) + b \frac{E_p}{E_0} \left(1 - \frac{e(V_p - V_B)}{E_p} \right)^2 \right]. \quad (6)$$

The total current of the probe I_t is

$$I_t(V_B) = I_{pl}(V_B) - I_{ep}(V_B) + I_{es}(V_B). \quad (7)$$

The experimental data and the theoretical calculation using Eq. (7) are compared in Fig. 6. The main discrepancy comes from the inaccurate estimation of the plasma electron density and temperature and the difference between the secondary electron emission coefficient of real tantalum disk probe and clean tantalum. It is hard to accurately subtract the plasma electron current and primary electron current from the affected *I-V* characteristic. $\sigma(E)$ of the real tantalum disk probe is higher than that of clean tantalum because the surface of the probe is dirty. Although the probe is cleaned by high-energy ion bombardment (the probe is biased at -600 V), the probe surface returns to dirty state within approximately 1 min.

ACKNOWLEDGMENT

This work was supported by NSF Grant No. ECS-8704529 and NASA Grant No. NAGW-275.

[1]F. F. Chen, *Plasma Diagnostic Techniques*, edited by R.H. Huddlestone and S. L. Leonard (Academic, New York, 1965).

[2]J. D. Swift and M. J. R. Schwar, *Electrical Probes for Plasma Diagnostics* (ILIFFE Books, London, 1970).

[3]J. P. Harbor, The Effect of Secondary Electron Emission on a Plasma Sheath, CLM-P 535 (1978) (unpublished).

[4]R. Limpaecher and K. R. MacKenzie, Rev. Sci. Instrum. **44**, 726 (1973).

[5]K. N. Leung, N. Hershkowitz, and K. R. MacKenzie, Phys. Fluids **19**, 1045 (1976).

[6]A. Lang and N. Hershkowitz, J. Appl. Phys. **49**, 4707 (1978).

[7]G. D. Hobbs and J. A. Wesson, Plasma Phys. **9**, 85 (1967).

[8]N. R. Whetter, in *Handbook of Chemistry and Physics*, 66th ed., edited by R. C. Weast (CRC, Cleveland, 1985-86), p. E-363.

[9]P. R. Warnecke, J. Phys. Rad. **7**, 270 (1936).

[10]O. Hachenberg and W. Brauer, *Advances in Electronics and Electron Physics*, edited by L. Martor (Academic, New York, 1959), Vol. XI, p. 413.

[11]E. Y. Wang, N. Hershkowitz, and T. Intrator, Rev. Sci. Instrum. **57**, 1085 (1986).

[12]N. Hershkowitz, in *Plasma Diagnostics*, edited by O. Auciello and D. Flamm (to be published).